



Technical Notes

Thermoelastic–Structural Analysis of Space Thin-Walled Beam Under Solar Flux

Zhenxing Shen*

Yanshan University, 066004 Qinhuangdao,
 People's Republic of China

and

Gengkai Hu†

Beijing Institute of Technology, 100081 Beijing,
 People's Republic of China

DOI: 10.2514/1.J057793

I. Introduction

THE uncoupled and coupled thermal–structural analysis models have been employed extensively to study thermally induced vibrations of spacecraft appendages [1–5]. The uncoupled model assumes that the absorbed solar flux for the structure surface is not affected by thermally induced motions (i.e., neglecting the coupling effect between structural deformations and incident heating); however, the coupled model includes the effect [1]. Furthermore, thermal flutter that is oscillations of increasing amplitude can be demonstrated by the coupled model and the stability analysis [1,6], and the unstable vibrations may cause spacecraft to experience such large motions and be unable to complete the intended missions [1]. For thermal–structural analysis, the heat conduction equation in thermal analysis is established based on the conservation of energy with neglect of the work done by external forces and the kinetic energy. According to the thermoelasticity theory, however, the strain rate coupling term exists in the heat conduction equation because the work should be included in the process of deriving the equation [7,8]. That is, the coupling effect between strain and temperature fields is considered in the thermoelastic–structural analysis.

This Note focuses on the investigation of stability of thermally induced vibrations and thermally induced dynamical behaviors of a space thin-walled beam subjected to thermal shock from solar flux using the thermoelastic–structural analysis. First, the heat conduction equation with the coupling effects mentioned in the preceding paragraph is derived by applying the principle of conservation of energy, the second law of thermodynamics, and Fourier's law in heat transfer; and the equation of motion with thermal effect is obtained by using Hamilton's principle and the approximating displacement field. Thermoelastic–structural coupling equations are then solved by an analytical approach similar to Ref. [1], which is to have a better

comparison between the presented analysis and the previous analysis in Ref. [1]. Finally, numerical results are conducted to illustrate the difference between thermoelastic–structural and thermal–structural analyses.

II. Thermoelastic–Structural Analysis

Thermally induced vibrations of a cantilevered thin-walled beam subjected to solar flux S_0 for time $t \geq 0$ (see Fig. 1) are studied by thermoelastic–structural analysis. In thermoelastic and structural analyses, the assumptions in Ref. [1] about thermal analysis and the Euler–Bernoulli beam theory are employed, respectively.

A. Derivation to Thermoelastic–Structural Equations

According to the first law of thermodynamics, for the heating elastic body per unit volume, the expression of conservation of energy is given by

$$da + di = \delta q + \delta g \quad (1)$$

where da and di are the increase of internal and kinetic energies, and δq and δg are the energy obtained by heat transfer and the work done by external forces, respectively. Based on the elasticity theory, Eq. (1) can be rewritten as

$$da - \delta q = \sigma_x d\epsilon_x \quad (2)$$

where σ_x and ϵ_x are the normal stress and strain along the x axis, respectively.

According to the definition of entropy in the second law of thermodynamics [9], $\delta q = Tde$, Eq. (2) may then be expressed as

$$da = Tde + \sigma_x d\epsilon_x \quad (3)$$

where T is the absolute temperature, and e is the entropy per unit volume. Defining the Helmholtz function $f = a - Te$ as given in thermodynamics [9], differentiating this function and then using Eq. (3) yields

$$df = \sigma_x d\epsilon_x - edT \quad (4)$$

Furthermore, f as a state function can be defined as $f = f(\epsilon_x, T)$. Differentiating the state function, and comparing with Eq. (4), one gets

$$\frac{\partial f}{\partial \epsilon_x} = \sigma_x \quad (5)$$

$$\frac{\partial f}{\partial T} = -e \quad (6)$$

In the linear elastic case, Hooke's law with temperature effect states

$$\sigma_x = E\epsilon_x - E\alpha_T(T - T_0) \quad (7)$$

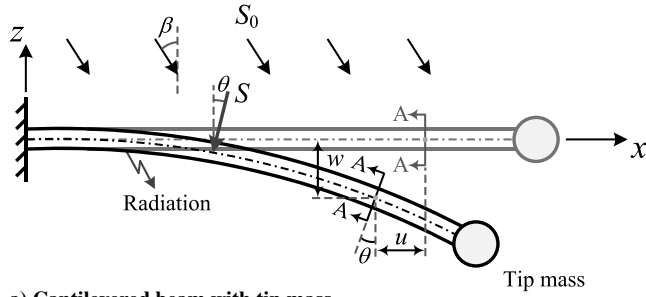
where E is Young's modulus, α_T is the coefficient of thermal expansion, and T_0 is the initial temperature as the reference value. Substituting the stress expression into Eq. (5) and then integrating this equation yields

$$f = \frac{1}{2} E\epsilon_x^2 - E\alpha_T(T - T_0)\epsilon_x + f_0(T) \quad (8)$$

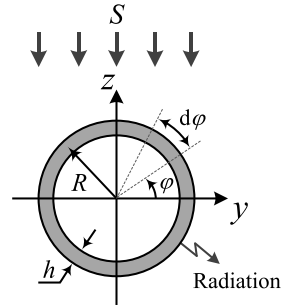
Received 6 August 2018; revision received 29 October 2018; accepted for publication 21 January 2019; published online 26 February 2019. Copyright © 2019 by the American Institute of Aeronautics and Astronautics, Inc. All rights reserved. All requests for copying and permission to reprint should be submitted to CCC at www.copyright.com; employ the eISSN 1533-385X to initiate your request. See also AIAA Rights and Permissions www.aiaa.org/randp.

*Lecturer, Key Laboratory of Mechanical Reliability for Heavy Equipment and Large Structures, Hebei Province, School of Civil Engineering & Mechanics; shenzx@ysu.edu.cn.

†Professor, Key Laboratory of Dynamics and Control of Flight Vehicle, Ministry of Education, School of Aerospace Engineering; hugeng@bit.edu.cn.



a) Cantilevered beam with tip mass



b) Cross-section A-A

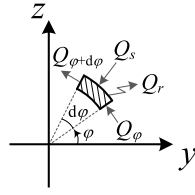

 c) Heat flux of segment $Rd\phi$

Fig. 1 Space thin-walled beam subjected to solar flux.

where f_0 is the Helmholtz function that is independent of strain. Substituting Eq. (8) into Eq. (6) leads to

$$e = E\alpha_T \varepsilon_x - \frac{\partial f_0}{\partial T} \quad (9)$$

Combining Eq. (9) and the definition of the specific heat at constant volume c_V [9], one obtains

$$c_V = \frac{T de}{\rho dT} \Big|_{\varepsilon_x = \text{const}} = -\frac{T}{\rho} \frac{\partial^2 f_0}{\partial T^2} \quad (10)$$

where ρ is the mass density. Then, integrating Eq. (10) with respect to T and substituting this equation into Eq. (9), one has

$$e = E\alpha_T \varepsilon_x + \rho c_V \ln \frac{T}{T_0} \quad (11)$$

Thus,

$$\frac{\delta q}{dt} = T \frac{de}{dt} = E\alpha_T T \dot{\varepsilon}_x + \rho c_V \dot{T} \quad (12)$$

where $\dot{\varepsilon}_x$ and \dot{T} are the rate of strain and temperature, respectively, and the constant-volume specific heat c_V can be replaced by the specific heat c for solids [9].

For the very small segment of thin-walled beam (see Fig. 1c), the energy per unit time obtained by heat transfer is

$$\frac{\delta q}{dt} dV = Q_\phi - Q_{\phi+d\phi} + Q_s - Q_r \quad (13)$$

where dV is the volume of a small segment. According to Fourier's law, the energy transfer by heat conduction can be defined as

$$Q_\phi - Q_{\phi+d\phi} = \frac{k}{R^2} \frac{\partial^2 T}{\partial \phi^2} dV \quad (14)$$

where k is the thermal conductivity. The absorbed solar flux Q_s and the radiant heat flux Q_r are given by

$$\begin{cases} Q_s = \delta(\alpha_s S \sin \phi)(Rd\phi dx) \\ Q_r = \sigma_T \varepsilon_T T^4 (Rd\phi dx) \end{cases} \quad (15)$$

where α_s is the surface absorptivity, σ_T is the Stefan–Boltzmann constant, ε_T is the surface emissivity, S is the projection of solar flux S_0 onto the line that is perpendicular to the beam axis (see Fig. 1a), and the parameter δ is used to define whether the tube surface suffers the solar flux (see Fig. 1b), that is,

$$\delta = \begin{cases} 1, & 0 \leq \phi \leq \pi \\ 0, & -\pi < \phi < 0 \end{cases} \quad (16)$$

Finally, the thermoelastic equation can be obtained by using Eqs. (12–16), as

$$\frac{\partial T}{\partial t} - \frac{k}{\rho c R^2} \frac{\partial^2 T}{\partial \phi^2} + \frac{\sigma_T \varepsilon_T}{\rho c h} T^4 + \frac{E\alpha_T}{\rho c} T \dot{\varepsilon}_x = \frac{\alpha_s S}{\rho c h} \delta \sin \phi \quad (17)$$

in which the rate of strain can be calculated from the following structural analysis. However, it is removed in thermal–structural analysis [1,6] due to the fact that the terms di and δg are neglected in Eq. (1).

For the structural analysis, the axial and bending deformations of the cantilevered beam are described approximately by the shape functions $N_a = x/l$ and $N_b = 0.5(3x^2/l^2 - x^3/l^3)$, respectively. The displacements of one point on the beam centerline can then be written as

$$\begin{cases} u(x, t) = N_a(x)U(t) \\ w(x, t) = N_b(x)W(t) \end{cases} \quad (18)$$

where U and W are the displacements at $x = l$, and l is the beam length. Based on the displacement field and using Hamilton's principle, the structural equations of the thin-walled beam with tip mass m are obtained as

$$\begin{cases} M_a \ddot{U} + K_a U = F_a(t) \\ M_b \ddot{W} + K_b W = F_b(t) \end{cases} \quad (19)$$

where

$$\begin{cases} M_a = \rho A \int_0^l N_a^2 dx + m \\ K_a = EA \int_0^l N_a'^2 dx \\ F_a = E\alpha_T \int_V N_a'(T - T_0) dV \end{cases} \quad (20)$$

and

$$\begin{cases} M_b = \rho A \int_0^l N_b^2 dx + m \\ K_b = EI_y \int_0^l N_b'^2 dx \\ F_b = -\int_0^l N_b' M_T(x, t) dx \end{cases} \quad (21)$$

in which the superscript $'$ refers to differentiation with respect to x , I_y is the cross-section moment of inertia, and M_T is the thermal moment [1,6].

Thermoelastic–structural analysis of the space thin-walled beam under solar flux can be performed by solving the coupling equations between Eqs. (17) and (19).

B. Solution to Thermoelastic–Structural Equations

To solve Eq. (17), the temperature distribution along the circumferential direction is approximated by means of a trigonometric function [1,3]:

$$T(x, \phi, t) = \bar{T}(x, t) + T_m(x, t) \sin \phi \quad (22)$$

where \bar{T} is the average temperature, and T_m is the perturbation temperature. And the term including δ in Eq. (17) is considered by Fourier series with neglect of higher-order terms:

$$\delta \sin \varphi = \frac{1}{\pi} + \frac{1}{2} \sin \varphi \quad (23)$$

Substituting Eqs. (22) and (23) into Eq. (17), then decoupling this equation by the weighted residual method, and using 1 and $\sin \varphi$ as the weight functions, respectively, one obtains

$$\begin{cases} \frac{\partial \bar{T}}{\partial t} + \frac{\sigma_T \varepsilon_T}{\rho c h} \bar{T}^4 + \frac{E \alpha_T}{\rho c l} \bar{T} \dot{U} - \frac{E \alpha_T R N_b'''}{2 \rho c} T_m \dot{W} = \frac{\alpha_s S}{\pi \rho c h} \\ \frac{\partial T_m}{\partial t} + \left(\frac{k}{\rho c R^2} + \frac{4 \sigma_T \varepsilon_T \bar{T}^3}{\rho c h} \right) T_m + \frac{E \alpha_T}{\rho c l} T_m \dot{U} - \frac{E \alpha_T R N_b'''}{\rho c} \bar{T} \dot{W} = \frac{\alpha_s S}{2 \rho c h} \end{cases} \quad (24)$$

To obtain the analytical solution for Eq. (24), we assume that the temperatures in these terms including \dot{U} and \dot{W} in Eq. (24) are constants [7,8], in which the perturbation temperature is the initial value 0 K because it is far smaller than the average temperature, and the average temperature is the steady-state value \bar{T}_{ss} [1,6]. In addition, the thermal characteristic time τ given in Ref. [1] is also used. Then, for the coupled models, Eq. (24) is rewritten as

$$\begin{cases} \frac{\partial \bar{T}}{\partial t} + \frac{\sigma_T \varepsilon_T}{\rho c h} \bar{T}^4 + \frac{E \alpha_T}{\rho c l} \bar{T}_{ss} \dot{U} = \frac{\alpha_s S_0}{\pi \rho c h} \cos(\beta + \theta) \\ \frac{\partial T_m}{\partial t} + \frac{1}{\tau} T_m - \frac{E \alpha_T R N_b'''}{\rho c} \bar{T}_{ss} \dot{W} = \frac{\alpha_s S_0}{2 \rho c h} \cos(\beta + \theta) \end{cases} \quad (25)$$

Because the purpose of this Note is to compare z -displacement responses with Ref. [1], in Eq. (25), one needs only to calculate T_m , whereas \bar{T} is not considered. The perturbation temperature equation, as a first-order linear differential equation, can be solved to yield

$$T_m = e^{-(t/\tau)} \int_0^t e^{(p/\tau)} \left(\frac{E \alpha_T R N_b'''}{\rho c} \bar{T}_{ss} \dot{W} + \frac{\alpha_s S_0}{2 \rho c h} \cos(\beta + \theta) \right) dp \quad (26)$$

where $\theta = -\partial w / \partial x$. Then, thermal moment in Eq. (21) can be obtained as

$$M_T = \frac{E I_y \alpha_T}{R} T_m \quad (27)$$

With damping, the equation of motion of tip z displacement becomes

$$\ddot{W} + 2\zeta \omega_0 \dot{W} + \omega_0^2 W = \frac{F_b(t)}{M_b} \quad (28)$$

where $\omega_0 = \sqrt{K_b/M_b}$ is the first-mode natural frequency, and ζ is the damping ratio. The applied load induced by thermal moment is expressed as

$$\begin{aligned} F_b(t) = e^{-(t/\tau)} & \left(C_1 \int_0^t e^{(p/\tau)} dp + C_2 \int_0^t e^{(p/\tau)} W dp \right. \\ & \left. + C_3 \int_0^t e^{(p/\tau)} \dot{W} dp \right) \end{aligned} \quad (29)$$

where

$$\begin{cases} C_1 = -\frac{E I_y \alpha_T \alpha_s S_0 \cos \beta}{2 \rho c h R} \int_0^l N_b'' dx \\ C_2 = -\frac{E I_y \alpha_T \alpha_s S_0 \sin \beta}{2 \rho c h R} \int_0^l N_b' N_b'' dx \\ C_3 = -\frac{E^2 \alpha_T^2 I_y \bar{T}_{ss}}{\rho c} \int_0^l N_b''^2 dx \end{cases} \quad (30)$$

After the Laplace transform for Eq. (28), one has

$$b(s)W(s) = \frac{1}{s} \frac{C_1}{M_b} \quad (31)$$

where $b(s)$ is the characteristic equation that is used to determine the stability of the solution:

$$b(s) = s^3 + \left(2\zeta \omega_0 + \frac{1}{\tau} \right) s^2 + \left(\omega_0^2 + \frac{2\zeta \omega_0}{\tau} - \frac{C_3}{M_b} \right) s + \left(\frac{\omega_0^2}{\tau} - \frac{C_2}{M_b} \right) \quad (32)$$

A dimensionless $b(s)$ is defined as

$$\bar{b}(s) = \bar{s}^3 + (2\zeta + \kappa) \bar{s}^2 + (1 + 2\zeta \kappa + \mu) \bar{s} + (\kappa + \kappa \eta) \quad (33)$$

where

$$\bar{s} = \frac{s}{\omega_0}, \quad \kappa = \frac{1}{\omega_0 \tau}, \quad \eta = -\frac{C_2}{K_b} \tau, \quad \mu = -\frac{C_3}{K_b} \quad (34)$$

Based on the Routh–Hurwitz stability criterion, the condition for a stable response is

$$\eta < \frac{2\zeta \kappa^2 + 4\zeta^2 \kappa + 2\zeta + (2\zeta + \kappa) \mu}{\kappa} \quad (35)$$

By comparing with Ref. [1], it can be found that the term including μ in Eq. (35) is added due to the thermoelasticity coupling effect. And the tip z -displacement responses $W(t)$ can be calculated by numerically solving the equation obtained by means of the inversion of the Laplace transform for $W(s)$.

Table 1 Four kinds of coupling analysis models

Analysis model	C_1	C_2	C_3
Coupled thermoelastic–structural	✓	✓	✓
Coupled thermal–structural	✓	✓	–
Uncoupled thermoelastic–structural	✓	–	✓
Uncoupled thermal–structural	✓	–	–

Table 2 Parameters of the thin-walled beam

Parameter	Value
S_0	1350 W/m ²
α_s	0.5
l	7.5 m
R	9.53×10^{-3} m
h	2.03×10^{-4} m
$E I_y$	84 N · m ²
α_T	1.69×10^{-5} K ⁻¹
ρ	8026 kg/m ³
m	1.5 kg
c	502 J/(kg · K)
k	16.6 W/(m · K)
ε_T	0.13
σ_T	5.67×10^{-8} W/(m ² · K ⁴)

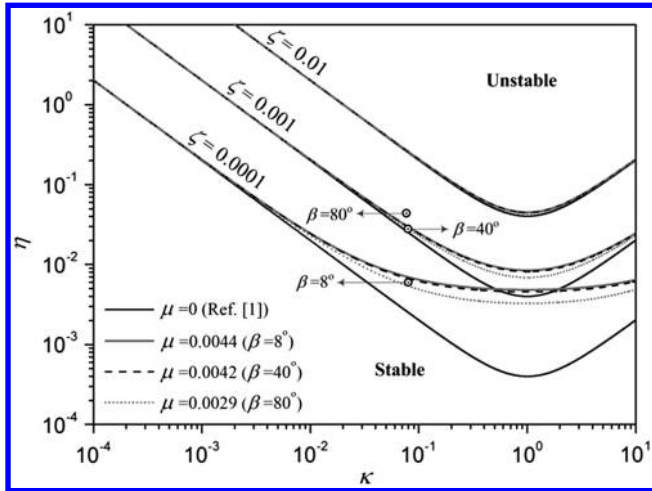


Fig. 2 Stability boundaries for the different ζ and μ .

III. Numerical Results

In the numerical simulations, thermally induced vibrations of the thin-walled beam under solar flux are analyzed by four kinds of models, as shown in Table 1, in which the coupled thermoelastic-structural and thermal-structural models consider the coupling effect between structural deformations and absorbed solar flux, and the uncoupled models neglect the effect. In addition, the symbols \surd and $-$ denote that the term including the constant C_1 , C_2 , or C_3 in

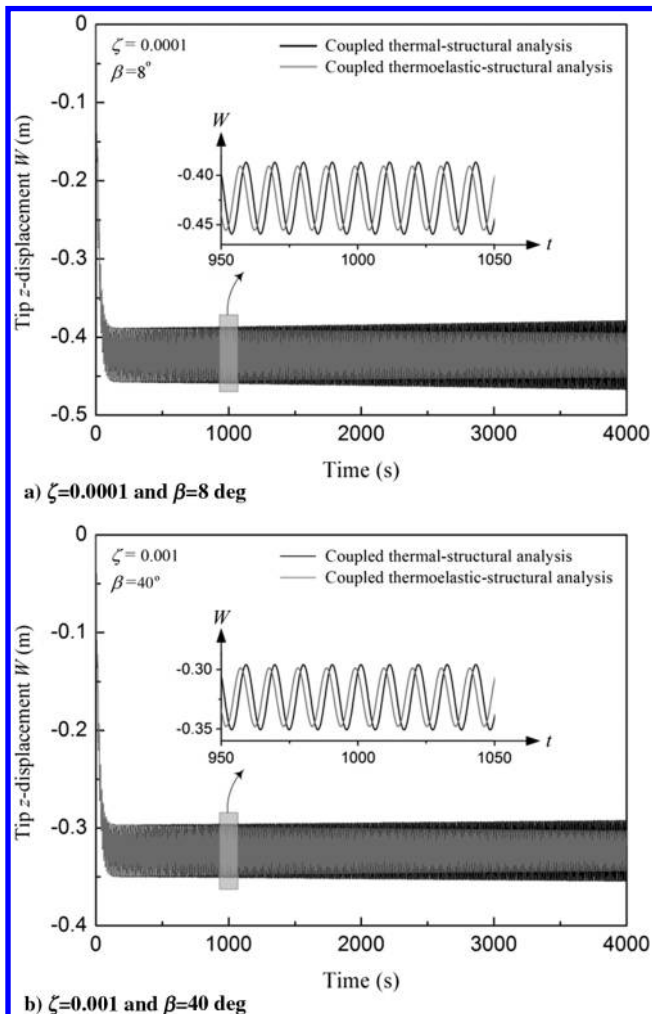


Fig. 3 Comparison of the dynamic responses for the two coupled models.

Eq. (29) is retained and removed for the different coupling analysis models, respectively.

Numerical results are first conducted to compare the difference in the stability criterion between the coupled thermoelastic-structural analysis and the coupled thermal-structural analysis. Based on the results of stability analysis, the tip z -displacement responses of the cantilevered beam at some certain solar incident angles β are then calculated by different models. The data used in the numerical calculations are listed in Table 2.

A. Stability Criterion

Using the stability criterion give in Eq. (35), it can be found that the system is always stable if the uncoupled models are adopted due to $C_2 = 0$ (see Table 1). However, the system may be unstable if the coupled models are employed and the design is above a stability boundary, as shown in Fig. 2. The three curves for the nondimensional parameter $\mu = 0$ are the same as Ref. [1], that is, the system is analyzed by the coupled thermal-structural model. The other nine curves for $\mu \neq 0$, which are the stability boundaries of coupled thermoelastic-structural analysis, in which μ with the different solar incident angle β is calculated using Table 2 data, have a significant difference with the coupled thermal-structural analysis when the system has a low damping ratio ζ and large nondimensional parameter κ . The results indicated that the thermoelasticity coupling effect plays an important role in the dynamics analysis of space thin-walled beam.

B. Dynamic Responses

Figure 3 presents the stable and unstable responses for two sets of ζ and β parameters chosen based on the stability criterion in Fig. 2. It is

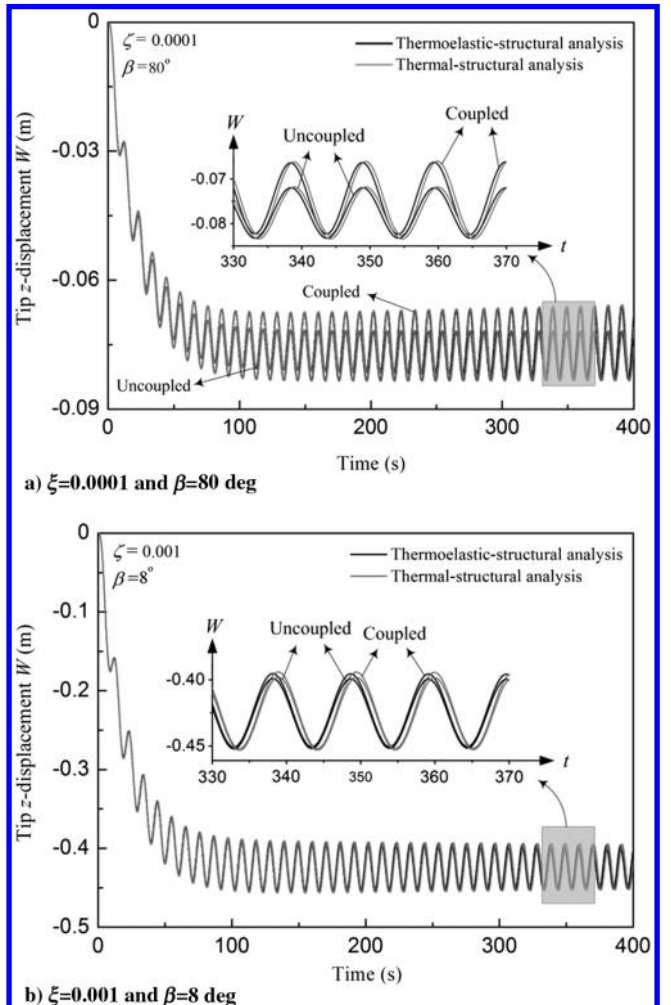


Fig. 4 Dynamic responses of the four kinds of analysis models.

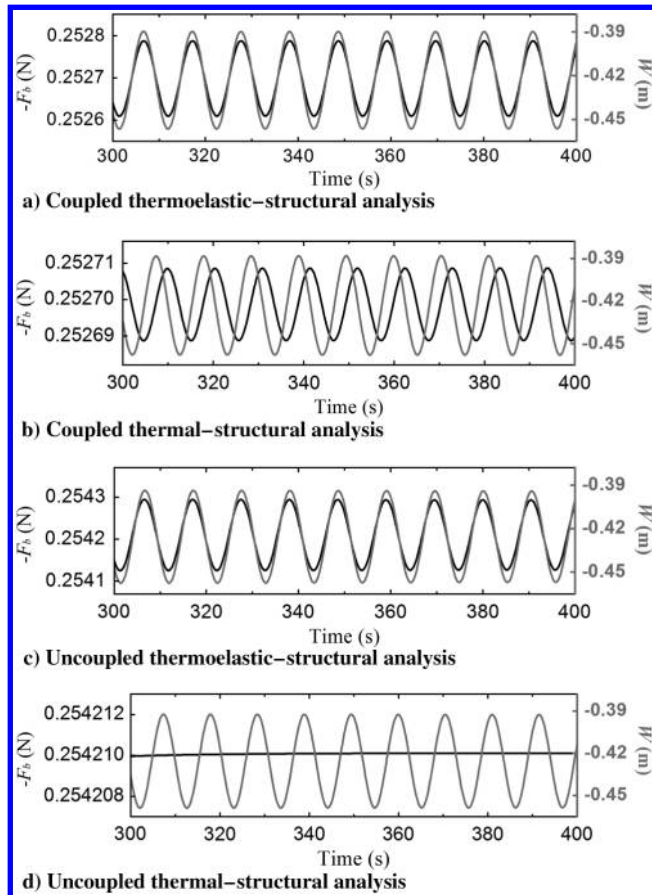


Fig. 5 Comparison of the phase between force and displacement responses with $\zeta = 0.0001$ and $\beta = 8$ deg.

clear that the dynamical characteristic of the thermally induced vibrations predicted by the coupled thermoelastic–structural analysis may be different from the coupled thermal–structural analysis. But the difference for dynamic responses within a short time is not significant.

To investigate the difference for the dynamic responses between thermoelastic–structural and thermal–structural analyses, without loss of generality, the responses of the two coupled models should both be stable or unstable, as shown in Fig. 4. It is observed that there is no significant difference in both uncoupled and coupled analyses within 400 s. In fact, the responses are computed at 4000 s; however, the differences for amplitude and phase become more obvious with the increase of time.

Moreover, to illustrate the physics cause of thermal flutter, Fig. 5 shows the force F_b in Eq. (29) and the tip z displacement W together. The parameters $\zeta = 0.0001$ and $\beta = 8$ deg are selected because thermal flutter can be observed only by the coupled thermal–structural analysis, and the responses of the other three analyses are all stable. As can be seen from Fig. 5, an obvious phase difference exists only in the coupled thermal–structural analysis, which results in the sum of work done by the thermal moment and damping force being positive, and then the amplitude of the vibration would increase continuously.

IV. Conclusions

Thermoelastic–structural analysis of a space thin-walled beam under solar flux is developed to illustrate the difference with thermal–structural analysis. By comparing the results of the two analyses, it is found that the difference for the stability boundaries may be significant; however, the dynamic responses within a short time are not obvious. Moreover, the physics cause of thermal flutter is the fact that a phase difference exists between force and displacement responses. The analytical method presented in this Note can obtain a more accurate stability criterion of the thermally induced vibrations of spacecraft appendages.

Acknowledgments

This work was supported by the National Natural Science Foundation of China under grant 11702241, the Natural Science Foundation of Hebei Province of China under grant A2017203272, and the Science and Technology Research Program in Higher Education of Hebei Province of China under grant QN2017149.

References

- [1] Thornton, E. A., and Kim, Y. A., “Thermally Induced Bending Vibrations of a Flexible Rolled-Up Solar Array,” *Journal of Spacecraft and Rockets*, Vol. 30, No. 4, 1993, pp. 438–448. doi:10.2514/3.25550
- [2] Ko, K. E., and Kim, J. H., “Thermally Induced Vibrations of Spinning Thin-Walled Composite Beam,” *AIAA Journal*, Vol. 41, No. 2, 2003, pp. 296–303. doi:10.2514/2.1943
- [3] Xue, M. D., Duan, J., and Xiang, Z. H., “Thermally-Induced Bending-Torsion Coupling Vibration of Large Scale Space Structures,” *Computational Mechanics*, Vol. 40, No. 4, 2007, pp. 707–723. doi:10.1007/s00466-006-0134-x
- [4] Shen, Z., and Hu, G., “Thermally Induced Dynamics of a Spinning Spacecraft with an Axial Flexible Boom,” *Journal of Spacecraft and Rockets*, Vol. 52, No. 5, 2015, pp. 1503–1508. doi:10.2514/1.A33116
- [5] Liu, L., Cao, D., Huang, H., Shao, C., and Xu, Y., “Thermal–Structural Analysis for an Attitude Maneuvering Flexible Spacecraft Under Solar Radiation,” *International Journal of Mechanical Sciences*, Vol. 126, June 2017, pp. 161–170. doi:10.1016/j.ijmecsci.2017.03.028
- [6] Zhang, J., Xiang, Z., Liu, Y., and Xue, M., “Stability of Thermally Induced Vibration of a Beam Subjected to Solar Heating,” *AIAA Journal*, Vol. 52, No. 3, 2014, pp. 660–665. doi:10.2514/1.J052574
- [7] Daneshjo, K., and Ramezani, M., “Classical Coupled Thermoelasticity in Laminated Composite Plates Based on Third-Order Shear Deformation Theory,” *Composite Structures*, Vol. 64, No. 3, 2004, pp. 369–375. doi:10.1016/j.compstruct.2003.09.039
- [8] Zhao, X., Hu, Q. J., Crossley, W., Du, C. C., and Li, Y. H., “Analytical Solutions for the Coupled Thermoelastic Vibrations of the Cracked Euler–Bernoulli Beams by Means of Green’s Functions,” *International Journal of Mechanical Sciences*, Vols. 128–129, Aug. 2017, pp. 37–53. doi:10.1016/j.ijmecsci.2017.04.009
- [9] Cengel, Y. A., and Boles, M. A., *Thermodynamics: An Engineering Approach*, 8th ed., McGraw–Hill, New York, 2015, Chaps. 4, 7, 12.

R. K. Kapania
Associate Editor